IOP Publishing Superconductor Science and Technology
Supercond. Sci. Technol. **27** (2014) 065019 (7pp) doi:10.1088/0953-2048/27/6/065019

Numerical simulation of the trapped field in MgB_2 bulk disks magnetized by field cooling

Hiroyuki Fujishiro, Tomoyuki Naito and Takafumi Yoshida

Faculty of Engineering, Iwate University, 4-3-5 Ueda, Morioka 020-8551, Japan

E-mail: fujishiro@iwate-u.ac.jp

Received 12 February 2014, revised 21 March 2014
Accepted for publication 1 April 2014
Published 15 May 2014

Abstract

We performed a numerical simulation of the trapped field properties of MgB_2 bulk disks with different superconducting characteristics magnetized by field cooling. The temperature dependence of the trapped field $B_z(T)$, and the time dependence of the local field $B_z(t)$ and temperature $T(t)$ were calculated, and compared with experimental results. Since the measured critical current density $J_c(T,B)$ was used in the simulation, the results of the simulation reproduce the experimental results well. These results suggest that the value of B_z and the trapped field profile can be estimated precisely for bulks of any shape and under any conditions, such as the operating temperature and applied field, using the measured $J_c(T,B)$ characteristics. The diameter and thickness dependence of B_z was also calculated.

Keywords: MgB_2, field-cooled magnetization, simulation

(Some figures may appear in colour only in the online journal)

1. Introduction

A superconducting bulk magnet using REBaCuO (RE: rare earth element or Y) material is one of the typical models for practical applications, such as sputtering cathodes, magnetic separation, drug delivery systems and so on [1], which produces quasi-permanent magnets on the order of several Tesla. However, it is difficult to fabricate single-domain REBaCuO bulk crystals larger than 100 mm in diameter because of the difficulties with crystal growth. MgB_2 bulk also has potential as a quasi-permanent magnet, and is attractive in a number of ways as it is low-cost, rare-earth-free and light-weight, and has a homogeneous trapped field distribution, which is in clear contrast to the distribution of an REBaCuO bulk magnet. Since the problem of weak links at the grain boundaries can be ignored in the MgB_2 polycrystal due to their long coherence length, ξ [2], better and larger polycrystalline MgB_2 bulk magnets can be achieved below the transition temperature $T_c = 39$ K. MgB_2 bulk magnets are expected to be applicable in magnetically levitated trains (MAGLEVs) [3] and wind power generators [4] using cryocooler cooling or as part of a liquid hydrogen economy in the near future. Several groups have fabricated MgB_2 bulks using different techniques, and reported the trapped field using field-cooled magnetization (FCM). At present, the maximum trapped field B_z reported has been 2.25 T at 15 K on a single MgB_2 bulk [5] and 3.14 T at 17.4 K in a bulk pair [6]. Pulsed-field magnetization (PFM) has also been investigated to magnetize the superconducting bulks because of its inexpensive and mobile setup without the need for a superconducting coil magnet [7, 8]. We have investigated the trapped field B_z by PFM on MgB_2 bulks fabricated by several techniques [9, 10]. However, the maximum trapped field was as low as 0.71 T at 15 K for a single MgB_2 bulk fabricated by a capsule method [10].

The trapped field characteristics of the superconducting bulks vary widely depending on the temperature and magnetic field dependence of the critical current density $J_c(T,B)$, which results from the strength and density of the vortex pinning centres. The $J_c(T,B)$ characteristics are usually estimated by $M-H$ hysteresis curves for small pieces cut from the bulk. The macroscopic J_c characteristics are evaluated by the trapped field $B_z(T)$ by FCM, because qualitatively, bulks with higher J_c are believed to trap a higher B_z. For REBaCuO bulks, the geometry effect on the trapped field by FCM was studied numerically using a sand-pile model and a Biot–Savart law, and was compared with the experimental results [11, 12]. The trapped field B_z and the profiles were

Table 1. Specification of the measured MgB_2 bulks.

Bulk	Diameter (d)	Thickness (t_B)	B_z^{max}	T_c	Mass density
Bulk-A	26 mm	6.5 mm	2.5 T at 13 K	38.5 K	95%
Bulk-B	30 mm	10 mm	1.9 T at 16 K	38.8 K	50%

calculated at a fixed temperature using the fixed $J_c(B)$ value, which suggested that the results of the simulation also reproduced the experimental results. However, the relationship between $J_c(T,B)$ and $B_z(T)$ has not been investigated quantitatively using numerical techniques. For the PFM process, the numerical simulation of the flux dynamics and heat generation for REBaCuO and MgB_2 bulks has been investigated to optimize the PFM procedure and to enhance the B_z value [9, 13, 14].

In the present paper, we perform the numerical simulation of the trapped field properties by FCM for homogeneous MgB_2 bulk disks with different trapped field characteristics. The temperature dependence of the trapped field $B_z(T)$, the trapped field profile, and the temperature rise of the bulk were calculated, and compared with experimental results. The diameter and thickness dependences of B_z for the MgB_2 bulks are also calculated.

2. Experimental procedure and results

Two MgB_2 superconducting bulks (hereafter, bulk-A and bulk-B) with different superconducting characteristics were used in this study. Bulk-A was fabricated by a hot isostatic pressing method; the precursor pellet was prepared by cold isostatic pressing at 196 MPa using mixed powders of Mg (99.5% in purity, ⩽180 μm in grain size) and B (99% in purity, 300 mesh in grain size) with a molar ratio of 1.0:2.0. The pellet was sealed under vacuum in a stainless steel container and was heated at 900 °C for 3 h at an isostatic pressure of 98 MPa. Bulk-B was fabricated by a capsule method, which is described in detail [15]. The specification of the bulks and the maximum trapped field by FCM are summarized in table 1.

A schematic view of the experimental setup for FCM is presented in figure 1. The MgB_2 bulk disk with a stainless steel ring was tightly mounted on the cold stage of a Gifford–McMahon cycle helium refrigerator. A Hall sensor (F W Bell, BHT 921) and a Cernox thermometer were adhered to the centre of the bulk surface. A static magnetic field of B_{ex} = 5 T was applied to the bulk above T_c using a cryo-cooled superconducting solenoid magnet (JASTEC JMTD-10T100) and the bulk was then field-cooled to T_s. Thereafter, the applied field was swept down to zero at a rate of −0.22 T min^{-1} and the time dependences of the trapped field $B_z(t)$ and the temperature $T(t)$ were recorded. The temperature dependence of the trapped field $B_z(T)$ was measured by a 'sweep method', that is, after the FCM procedure at T_s, the bulk was warmed slowly with a heating rate of 0.1 K min^{-1} and the trapped field $B_z(T)$ was measured. Figure 2 shows the time dependences of the local field $B_z(t)$ and temperature $T(t)$ of bulk-A during FCM at T_s = 13 K. As the external field B_{ex} decreases, B_z also decreases and reaches a final value. The temperature T gradually increases about 0.8 K, reaches a maximum at the time at which B_{ex} becomes zero, and decreases with increasing time. Figure 3 shows the experimental results for $B_z(T)$ for both bulks. $B_z(T)$ for bulk-A was larger than that of bulk-B. The maximum B_z for bulk-A and bulk-B was 2.5 T at 13 K and 1.9 T at 16 K, respectively.

After the magnetizing experiments, the bulks were cut and small pieces about 1 × 1 × 2 mm^3 in size were prepared for magnetization curve $M(H)$ measurements at 10 and 20 K under a magnetic field up to $\mu_0 H$ = 5 T using a commercial SQUID magnetometer (MPMS-5 T; Quantum Design). The $J_c - B$ relationship was estimated from the $M(H)$ hysteresis loop using the extended Bean model, $J_c = 20\ \Delta M/a(1\text{-}a/3b)$, where a and b are the dimensions of the plane of the sample perpendicular to the applied field and ΔM is the width of the $M(H)$ loop. Figure 4 depicts the estimated $J_c - B$ characteristics for both bulks at 10 and 20 K.

3. Modeling and numerical simulation

Based on our experimental setup for FCM shown in figure 1, the framework for the numerical simulation was constructed [13]. In the model analysis, we include a thin spacing plate between the bulk and the cold stage with thermal conductivity κ_{CT} from 5 × 10^{-4} to 5 × 10^{-1} W K^{-1} m^{-1}, which represents both the cooling power of the refrigerator and the thermal contact. A static magnetic field of B_{ex} = 5 T was applied to the bulk above T_c using a solenoid magnet of inner diameter 120 mm, outer diameter 150 mm and height 100 mm, and the bulk was then field-cooled to T_s. A descending field $B_{ex}(t)$ was applied at a rate from −0.052 to −5.2 T min^{-1}. The physical phenomena occurring during FCM are described using the fundamental electromagnetic and thermal equations in axisymmetric coordinates.

$$\frac{\partial}{\partial r}\left[\frac{\nu}{r}\frac{\partial}{\partial r}(r\boldsymbol{A})\right] + \frac{\partial}{\partial z}\left(\nu\frac{\partial \boldsymbol{A}}{\partial z}\right) = J_0 + J \tag{1}$$

$$\rho C\frac{\partial T}{\partial t} = \frac{1}{r}\frac{\partial}{\partial r}\left(r\kappa\frac{\partial T}{\partial r}\right) + \frac{\partial}{\partial z}\left(\kappa\frac{\partial T}{\partial z}\right) + Q. \tag{2}$$

Here, $\boldsymbol{A}$ represents the magnetic vector potential, J_0 is the forced current density or coil current density and J denotes the superconducting current density or induced current density. In equation (2), κ, C and ρ, respectively, denote the thermal conductivity, the specific heat and the mass density

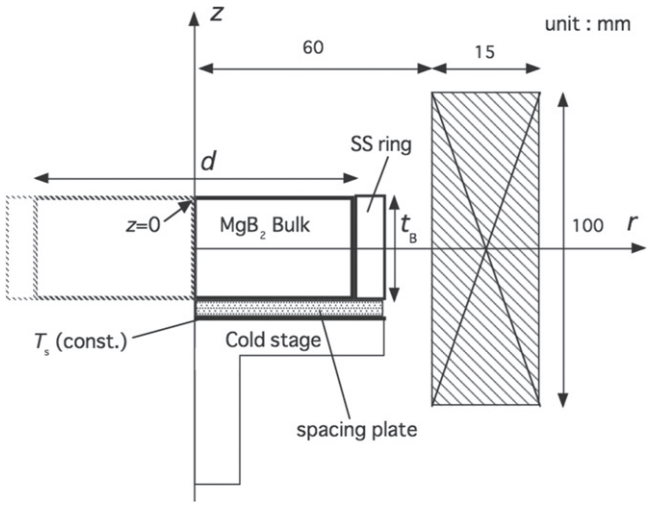

Figure 1. Schematic view of the experimental setup and the basis for the numerical model of FCM.

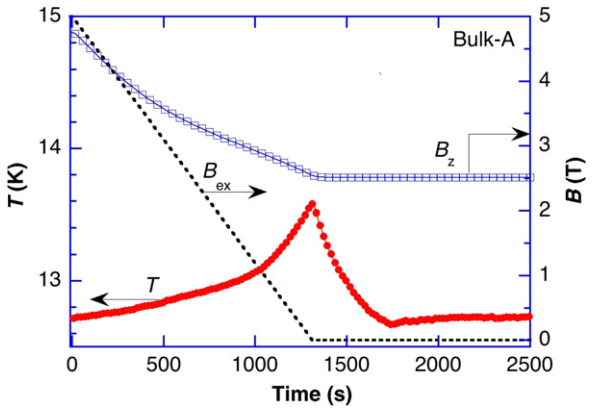

Figure 2. Experimental results of the time dependence of the local field $B_z(t)$ and temperature $T(t)$ at the centre of the surface of bulk-A during FCM at T_s = 13 K, when the external field $B_{ex}(t)$ was decreased at a rate of −0.22 T/min from 5 to 0 T.

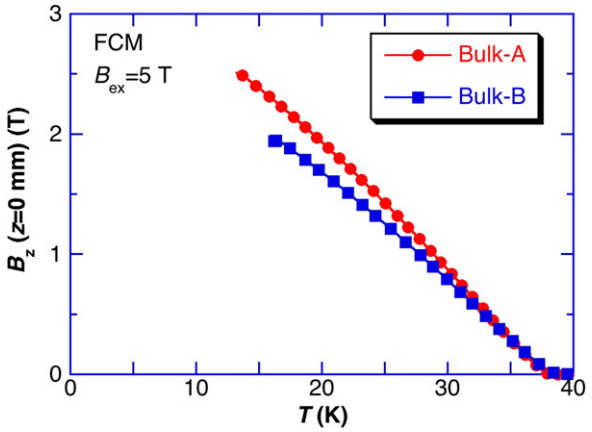

Figure 3. Experimental results of the trapped field $B_z(T)$ for both bulks magnetized by FCM.

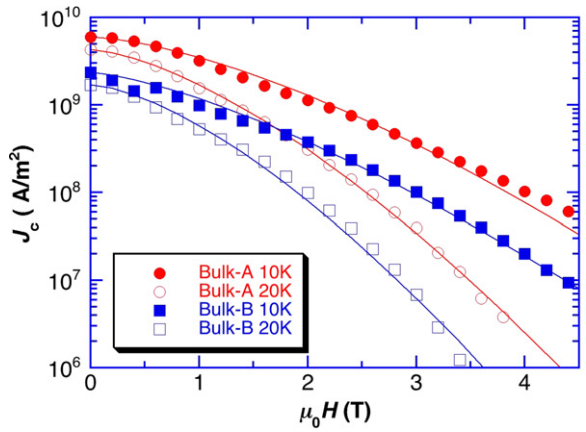

Figure 4. The estimated $J_c - B$ characteristics for both bulks at 10 and 20 K. The solid lines show the fitting curves used in the simulation (see text).

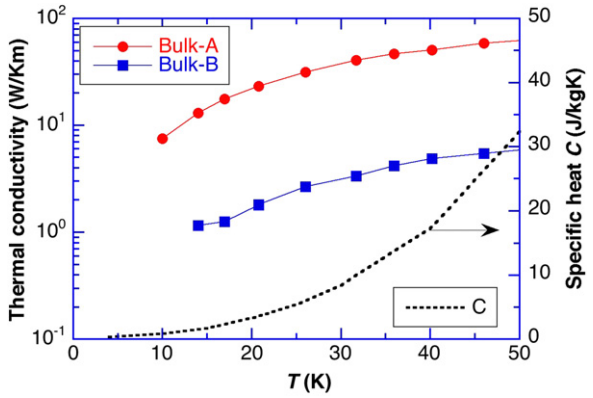

Figure 5. Thermal conductivity and specific heat of the MgB_2 bulks used in the simulation.

(=2590 kg m^{-3}) of the MgB_2 bulks. Figure 5 shows the temperature dependence of κ and C for the MgB_2 bulks used in the simulation, in which $\kappa(T)$ of both bulks was measured and $C(T)$ was referred from [16].

The J value is given as

$$J = \sigma E = -\sigma \frac{\partial A}{\partial t}, \tag{3}$$

where E is the electric field and σ the electric conductivity.

The power-n model (n = 100) was used to describe the nonlinear E-J characteristic of the superconducting bulk:

$$E = E_c \left(\frac{J}{J_c} \right)^n, \tag{4}$$

where J_c is the critical current density and $E_c(1 \times 10^{-6}$ V m$^{-1})$ is the reference electric field. In equation (2), heat generation Q in the bulk is given as $Q = JE$.

The magnetic field dependence of critical current density $J_c(B)$ for each bulk at 10 and 20 K was fitted, as shown in figure 4, using the following relation [17],

$$J_c(B) = J_{c0} \exp \left[-\left(\frac{B}{B_0} \right)^a \right], \tag{5}$$

where B_0 and a are the fitting parameters, which are summarized in table 2. The temperature dependence of J_{c0} under zero field is described by the following equation,

$$J_{c0} = \alpha \left\{ 1 - \left(\frac{T}{T_c} \right)^2 \right\}^{\frac{3}{2}}, \tag{6}$$

where T_c is the critical temperature (=39 K) and α is a constant representing J_c at 0 K. Iterative calculations were performed to obtain convergence of σ in the superconductor at each time step. Commercial software, Photo-Eddy, combined with Photo-Thermo (Photon Ltd, Japan), was used for analyzing the combined problem of electromagnetic fields and heat diffusion using the finite element method.

4. Results of simulation and discussion

4.1. Simulation under experimental conditions

Firstly, the results of the simulation during FCM are presented under the experimental conditions with the descending field of −0.22 T min^{-1}. Figure 6(a) shows the trapped field at the centre of the bulk surface $B_z(z = 0$ mm) as a function of temperature at 10 and 20 K for each bulk. In this figure, the experimental results for bulk-A and bulk-B are also shown. The results of the simulation reproduce the experimental results well. The slight difference between experiments and simulation may result from the inhomogeneity of $J_c(B)$ in the bulk and/or the temperature distribution in the bulk.

Table 2. Fitting parameters for the $J_c - B$ characteristics of each bulk.

Bulk	T_s	J_{c0} (A/m^2)	B_0 (T)	a in eqn (5)	α (A/m^2) in eqn (6)
Bulk-A	10 K	6.01×10^9	1.50	1.50	6.70×10^9
	20 K	4.31×10^9	1.05	1.50	
Bulk-B	10 K	2.36×10^9	1.30	1.40	2.70×10^9
	20 K	1.71×10^9	0.95	1.50	

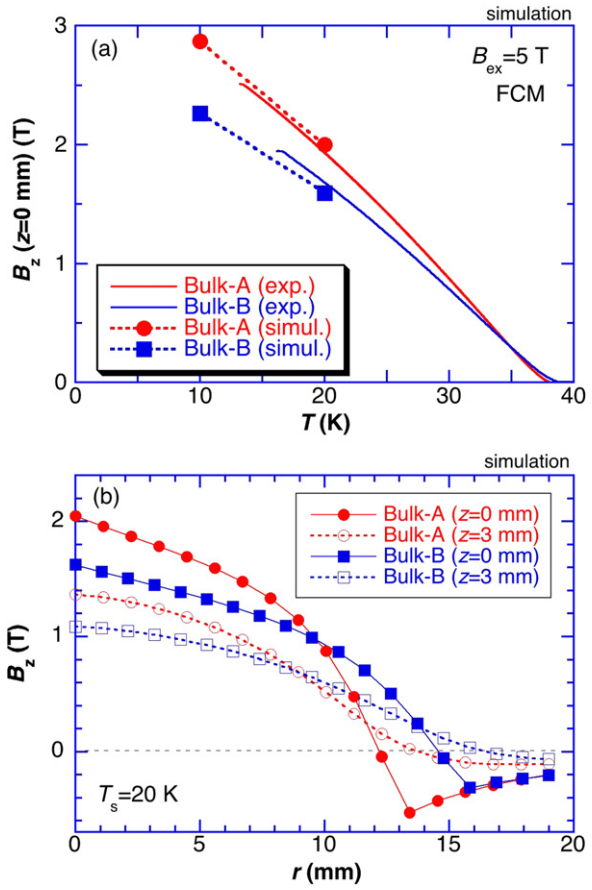

Figure 6. (a) The results of the simulation of the trapped field B_z (z = 0 mm) at 10 and 20 K for each bulk. Solid lines show the experimental results. (b) Cross-sections of the trapped field profiles at 20 K for each bulk at z = 0 (bulk surface) and 3 mm.

Figure 6(b) shows the cross-section of the trapped field profile $B_z(r)$ at z = 0 mm (bulk surface) and 3 mm. During FCM, the magnetic field in the bulk decreased with decreasing external field $B_{ex}(t)$ and a bell-shaped trapped field profile materializes, which may originate from the steep magnetic field dependence of J_c. These results are in contrast with those using Bean's critical state model, which results in a conical profile. At z = 3 mm, the absolute value of B_z decreases and the profiles become flatter. In this way, the trapped field and the profiles can be estimated at any

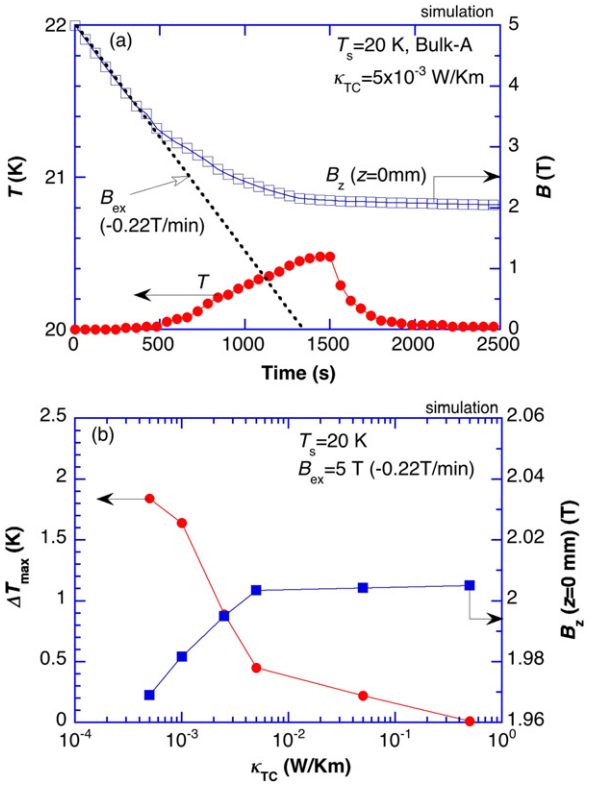

Figure 7. (a) Maximum temperature rise ΔT_{max} and final trapped field B_z ($z = 0$ mm) as a function of the thermal contact conductivity κ_{TC} at 20 K for bulk-A. (b) Time dependence of temperature $T(t)$ and local field $B_z(t)$ ($z = 0$ mm) at the centre of the bulk surface for $\kappa_{TC} = 5 \times 10^{-3}$ W K^{-1} m^{-1} at 20 K.

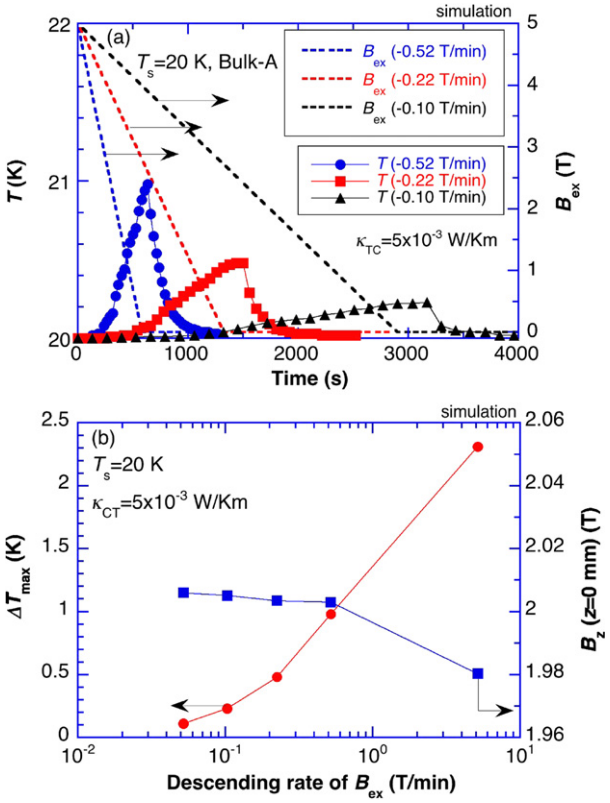

Figure 8. (a) Time dependence of the temperature $T(t)$ for descending B_{ex} rates of −0.52, −0.22 and −0.10 T min^{-1}. (b) Maximum temperature rise ΔT_{max} and final trapped field as a function of the descending B_{ex} rate during FCM.

position (z, r) and at any temperature T_s using the simulation.

Figure 7(a) depicts the results of the simulation of the time dependence of the temperature $T(t)$ and the local field $B_z(t)$ at the centre of the bulk surface during FCM for bulk-A at 20 K for a spacing plate with thermal conductivity $\kappa_{TC} = 5 \times 10^{-3}$ W K^{-1} m^{-1}. $T(t)$ gradually increases with decreasing $B_{ex}(t)$, takes a maximum of 20.5 K just after the time at which B_{ex} becomes zero, and recovers towards the initial temperature as time increases. The local field $B_z(t)$ decreases according to the decrease in $B_{ex}(t)$ for $t \leqslant 500$ s, but with increasing time, $B_z(t)$ approaches a final value of about 2 T according to pinning effects, which are reflected in the $J_c - B$ characteristics of the bulk. The results of the simulation qualitatively reproduce the experimental results shown in figure 2. Even in the FCM process, a small temperature rise occurs due to the slow movement of magnetic flux in the superconductor, which is much smaller than that seen during the PFM process with a time scale of milliseconds [18].

The temperature rise during FCM is supposed to vary largely depending on the κ_{TC} value used in the simulation. Figure 7(b) shows the maximum temperature rise ΔT_{max} and final trapped field B_z(final), as a function of κ_{TC}. ΔT_{max} increases adiabatically with decreasing κ_{TC}. As a result, B_z (final) slightly decreases with decreasing κ_{TC}, which is a reasonable result. Using figure 7(b), κ_{TC} in the present experimental setup, which represents both the cooling power of the refrigerator and the thermal contact, can be roughly estimated to be 3×10^{-3} W K^{-1} m^{-1}.

Figure 8(a) presents the results of the simulation of the time dependence of the temperature $T(t)$ for various descending rates of $B_{ex}(t)$ during FCM for bulk-A at 20 K under the condition of $\kappa_{TC} = 5 \times 10^{-3}$ W K^{-1} m^{-1}. Figure 8(b) shows the maximum temperature rise ΔT_{max} and final trapped field B_z (final), as a function of the descending rate of B_{ex}. ΔT_{max} increases with an increasing rate of descending B_{ex} and, as a result, the value of B_z (final) is decreased slightly. In this way, using the numerical simulation, the maximum temperature rise ΔT_{max} and final trapped field B_z (final) can be estimated for various κ_{TC} and descending rates of $B_{ex}(t)$. However, ΔT_{max} is relatively small due to the small C and high κ values of the MgB_2 bulk compared with those for REBaCuO bulks [19], and the influence of the temperature rise on the B_z (final) value is also quite small during FCM.

4.2. Thickness and diameter dependence of the trapped field

Using the numerical simulation, the magnitude and profile of the trapped field can be estimated for bulks with any

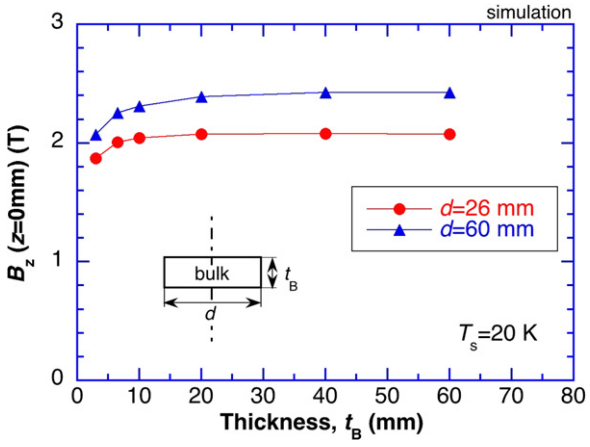

Figure 9. Results of the simulation of the thickness dependence of the trapped field B_z (z = 0 mm) at the centre of MgB_2 bulk disks of 26 mm and 60 mm in diameter.

dimension without experiments. In this subsection, the thickness and diameter dependence of the trapped field of the bulk disk is estimated, using the $J_c - B$ profile of the bulk-A in the simulation, with the temperature of the bulk fixed at T_s = 20 K because the temperature rise during FCM is fairly small, as shown in the previous section. Figure 9 shows the thickness (t_B) dependence of the trapped field B_z (z = 0 mm) at the centre of MgB_2 bulk disks of diameter d = 26 mm and 60 mm. B_z (z = 0 mm) increases with increasing thickness of the bulk for $t_B \leqslant$ 20 mm, but is independent of the value of t_B for thicker samples.

Figure 10(a) presents the diameter (d) dependence of the trapped field B_z (z = 0 mm) at the centre of an MgB_2 bulk disk of t_B = 6.5 mm. Figure 10(b) shows the cross-section of the trapped field profile $B_z(r)$ at z = 0 mm (bulk surface) of the bulk for various diameters. B_z (z = 0 mm) gradually increases with increasing diameter of the bulk, but this effect of diameter on the value of B_z is not so prominent; for example, B_z (z = 0 mm) for the d = 100 mm bulk is only 24% larger than that calculated for the d = 20 mm bulk, even though the diameter has increased five-fold. In figure 10(a), the experimental results for bulks with identical $J_c - B$ characteristics are also shown. The experimental results coincide with the results of the simulation. The diameter dependence of B_z comes from the steep $J_c - B$ characteristic, that is, J_c reduces significantly with increasing applied magnetic field. For Bean's model, B_z increases linearly with increasing diameter of the bulk. From these results, in the MgB_2 bulk, increasing the t_B and d values is not a valuable solution to enhance the B_z value, similar to REBaCuO bulks. Also for MgB_2 bulks, the improvement of the $J_c - B$ characteristic is only a possible solution to enhance the B_z value. If the $J_c - B$ at the mid-field region is enhanced and does not decay rapidly under an external field at lower temperature (e.g. 10 K), higher trapped fields in larger diameter samples can be obtained.

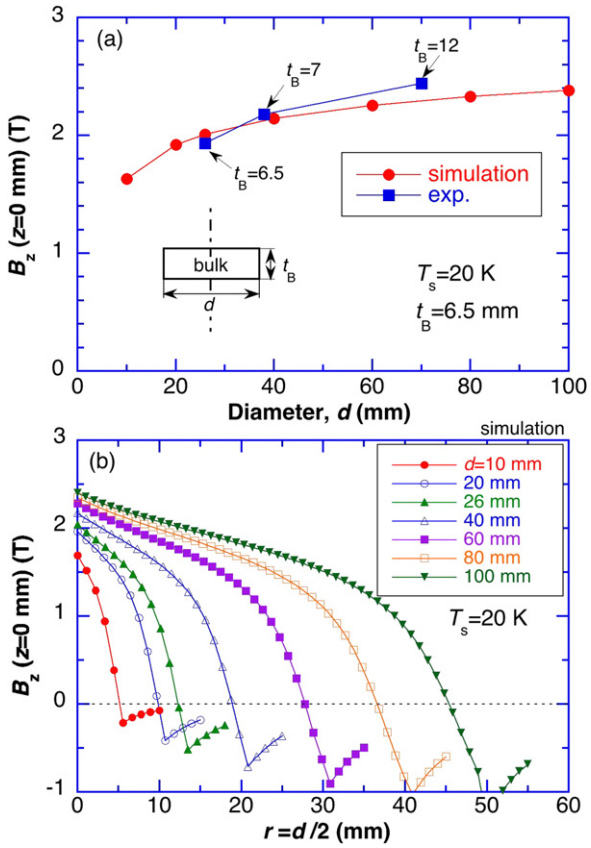

Figure 10. (a) Diameter dependence of the trapped field B_z (z = 0 mm) at the centre of the MgB_2 bulk disk of thickness 6.5 mm. The experimental results are also shown. (b) Cross-section of the trapped field profile $B_z(r)$ at z = 0 mm (bulk surface) of bulks with various diameters.

5. Summary

A numerical simulation of electromagnetic and thermal properties has been performed for cryo-cooled MgB_2 bulk discs magnetized by field cooling, and the simulation results are compared with the experimental results. The important results and conclusions obtained from this study are summarized as follows.

(1) Since measured critical current density $J_c(T,B)$ profiles were used in the simulation, the results of the simulation reproduce the experimental results well. These results suggest that the value of B_z and the trapped field profile can be estimated precisely for the bulk of any shape under various conditions, such as operating temperature and applied field, using the measured $J_c(T,B)$ characteristics.

(2) The diameter and thickness dependence of B_z was calculated for MgB_2 bulks of various diameters and thicknesses. The diameter of the bulk did not have a significant effect on the value of B_z; for example, B_z (z = 0 mm) for d = 100 mm bulk is only 24% larger than that for d = 20 mm bulk, even though the diameter has

increased five-fold. Increasing the thickness of the MgB_2 bulk is not very effective in enhancing the value of B_z. For MgB_2 bulks, improving the $J_c - B$ characteristic is a possible way to enhance the B_z value.

Acknowledgments

This work was supported in part by JSPS KAKENHI grant number 23560002, JST A-STEP (AS232Z02579B), and Hitachi Metals Materials Science Foundation.

References

[1] Oka T 2007 *Physica* C **463–465** 7
[2] Kambara M, Babu N H, Sadki E S, Cooper J R, Minami H, Cardwell D A, Campbell A M and Inoue I H 2001 *Supercond. Sci. Technol.* **14** L5
[3] Schultz L, de Haas O, Verges P, Beyer C, Rohling S, Olsen H, Kuhn L, Berger D, Noteboom U and Funk U 2005 *IEEE Trans. Appl. Supercond.* **15** 2301
[4] Ohsaki H, Terao Y and Sekino M 2010 *J. Phys. Conf. Series* **234** 032043
[5] Yamamoto A, Yumoto H, Shimoyama J, Kishio K, Ishihara A and Tomita M 2010 *Proc. Abstract 23rd Int. Symp. Supercond.* p 219
[6] Durrell J H, Dancer C E J, Dennis A, Shi Y, Xu Z, Campbell A M, Hari N, Todd R I, Grovenor C R M and Cardwell D A 2012 *Supercond. Sci. Technol.* **25** 112002
[7] Yanagi Y, Itoh Y, Yoshikawa M, Oka T, Ikuta H and Mizutani U 2005 *Supercond. Sci. Technol.* **188** 839
[8] Fujishiro H, Tateiwa T, Fujiwara A, Oka T and Hayashi H 2006 *Physica* C **445–448** 334
[9] Fujishiro H, Tamura T, Arayashiki T, Oyama M, Sasaki T, Naito T, Giunchi G and Albisetti A F 2012 *Jpn. J. Appl. Phys.* **51** 103005
[10] Fujishiro H, Naito T, Sasaki T and Arayashiki T 2010 *Proc. ICEC 24-ICMC 2012* p 571
[11] Aydiner A and Yanmaz E 2005 *Supercond. Sci. Technol.* **18** 1010
[12] Fukai H, Tomita M, Murakami M and Nagamoto T 2002 *Supercond. Sci. Technol.* **15** 1054
[13] Fujisiro H and Naito T 2010 *Supercond. Sci. Technol.* **23** 105021
[14] Xu Z, Levin R, Canpbell A M, Cardwell D A and Jones H 2012 *Supercond. Sci. Technol.* **25** 025016
[15] Naito T, Sasaki T and Fujishiro H 2012 *Supercond. Sci. Technol.* **25** 095012
[16] Wang Y, Plackowski J and Junod A 2001 *Physica* C **355** 179
[17] Xiang F X, Wang X L, Xun X, Silva K S B De, Wang Y X and Dou S X 2013 *Appl. Phys. Lett.* **102** 152601
[18] Fujishiro H, Naito T, Oyama M, Arayashiki T, Tamura T, Sasaki T and Giunchi G 2013 *IEEE Trans. Appl. Supercond.* **23** 6800804
[19] Oka T, Yokoyama K, Fujishiro H, Kaneyama M and Noto K 2005 *Physica* C **426–431** 794